Comparative analysis of Granger causality and transfer entropy to present a decision flow for the application of oscillation diagnosis

Brian Lindner, Lidia Auret, Margret Bauer, and J.W.D Groenewald

***Abstract*—Causality analysis techniques can be used for fault diagnosis in industrial processes. Multiple causality analysis techniques have been shown to be effective for fault diagnosis [1]. Comparisons of some of the strengths and weaknesses of these techniques have been presented in literature [2], [3]. However, there are no clear guidelines on which technique to select for a specific application. These comparative studies have not thoroughly addressed all the factors affecting the selection of techniques. In this paper, these two techniques are compared based on their accuracy, precision, automatability, interpretability, computational complexity, and applicability for different process characteristics. Transfer entropy and Granger causality are popular causality analysis techniques, and therefore these two are selected for this study. The two techniques were tested on an industrial case study of a plant wide oscillation and their features were compared. To investigate the accuracy and precision of Granger causality and transfer entropy, their ability to find true connections in a simulated process was also tested. Transfer entropy was found to be more precise and the causality maps derived from it were more visually interpretable. However, Granger causality was found to be easier to automate, much less computationally expensive, and easier to interpret the meaning of the values obtained. A decision flow was developed from these comparisons to aid users in deciding when to use Granger causality or transfer entropy, as well as to aid in the interpretation of the causality maps obtained from these techniques.**

***Index Terms*—Transfer entropy, Granger causality, causality analysis, fault diagnosis, plant wide oscillation, root cause diagnosis.**

I. Introduction

FAULT diagnosis, the detection and root cause identification of an abnormal event, is a complex and time-consuming task. Reis and Gins [4] highlighted improvements in the speed and accuracy of fault diagnosis as providing the most immediate potential benefit from monitoring of industrial processes. Causality analysis techniques can be used for data-based fault diagnosis. In these techniques, causal connections between measured variables are inferred. Since the symptoms of a fault will propagate through the process along these causal connections, the inferred causal connections can give an indication of the propagation path of the fault through the process. A number of variations of causality analysis have been researched for fault diagnosis, including: transfer entropy [5]–[13]; Granger causality [14]–[16]; cross-correlation [17]; partial directed coherence [14], [16]; and convergent cross-mapping [18]. This multitude of techniques can cause decision paralysis, where it is difficult to decide which of the techniques is appropriate for an engineer to use in a specific situation.

Duan et al. [3] demonstrated and compared different techniques for root cause diagnosis of plant wide oscillations. Granger causality and transfer entropy were the data-based causality analysis techniques they compared, and some of their advantages and disadvantages were listed. They found that Granger causality is easier to implement, robust to data selection, has low computational burden, and its application techniques are well developed. However, it is only suitable for linear relationships between variables, and may be prone to model misspecification. They also found that transfer entropy is robust to data selection, suitable for both linear and nonlinear relationships. However, it is sensitive to calculation parameter selection, difficult to implement, and the computational burden is large. Kühnert [19] provided guidelines for technique selection based on process characteristics. However, the guidelines were based on simulated experiments, and only the accuracy of the techniques was considered. Investigation of other factors is important. This shows that the different methods have varying strengths and weaknesses, and each may be uniquely suited to different applications.

This means that an exhaustive comparison of each technique will not completely remove the ambiguity of the decision between the methods. However, a comparative analysis can provide a decision-making framework to simplify the future application of these techniques in an industrial setting. The point of departure for this comparative analysis is to compare the two most popular techniques, Granger causality and transfer entropy. These two techniques have been proven effective at root cause diagnosis in industrial processes by numerous authors [5]–[12], [14], [15], [21]. Their wide-spread application in literature means that transfer entropy and Granger causality are mature techniques. This paper compares transfer entropy and Granger causality based on their accuracy, precision, automatability, interpretability, computational complexity, and applicability for different process characteristics.

The outline of this article is as follows. In Section II, the use of transfer entropy and Granger causality for root cause

This work was supported by Anglo American Platinum.

B. Lindner and L. Auret were with the Department of Process Engineering, Stellenbosch University, Matieland 7602, South Africa. They are now with Stone Three Digital, Somerset West, South Africa (e-mail: blindner@sun.ac.za; lauret@sun.ac.za).

M. Bauer is with the Department of Electrical, Electronic and Computer Engineering, University of Pretoria, Pretoria 0002, South Africa. (email: margret.bauer@up.ac.za.)

J.W.D. Groenewald is with Anglo American Platinum Limited, Johannesburg, South Africa

diagnosis is explained. In Section III, the features of Granger causality and transfer entropy are compared. In Section IV, the accuracy and precision of Granger causality and transfer entropy are tested and compared using a simulated case study. In Section V a decision flow for application of Granger causality or transfer entropy based on the findings of the paper is presented. In Section VI, these features and the presented decision flow are illustrated on an industrial case study of a plant wide oscillation. Finally, in Section VII, the conclusions of the paper are presented along with recommendations for future work.

II. Background on causality analysis for fault diagnosis

Causality analysis techniques infer the cause and effect relationships between measured variables from the historical time series data of the variables. The two causality analysis techniques discussed in the paper are described in this section.

A. Transfer entropy

Transfer entropy is an information-theoretic interpretation of Wiener's causality definition [22]. The transfer entropy from X to Y can be calculated as shown in Equation 1.

$$T_{y|x} = \sum p(y_{i+H}, \mathbf{y}_i^{(K)}, \mathbf{x}_i^{(L)}) \cdot \log \frac{p(y_{i+H}|\mathbf{y}_i^{(K)}, \mathbf{x}_i^{(L)})}{p(y_{i+H}|\mathbf{y}_i^{(K)})} \quad (1)$$

where: $\mathbf{x}_i^{(K)} = [x_i, x_{i-\tau}, ..., x_{i-(K-1)\tau}]$ and $\mathbf{y}_i^{(L)} = [y_i, y_{i-\tau}, ..., y_{i-(L-1)\tau}]$ are the embedded vectors of X and Y with embedding dimensions, K and L respectively, and time interval, τ; H is the prediction horizon. $p(.,.)$ represents the joint probability density function (PDF). The PDF can be estimated using empirical distribution fitting, such as kernel density estimation [23]. The transfer entropy represents the reduction in uncertainty of variable Y given past values of variable X. A causality measure can then be calculated by subtracting the influence of X given Y from the influence of Y given X [5].

$$T_{x \to y} = T_{y|x} - T_{x|y} \quad (2)$$

Uncertainty inherent in process measurements means that non-zero transfer entropy values will be calculated even when there is no causal relationship. A hypothesis test is performed to determine the statistical significance of each transfer entropy value. This can be done using the Monte Carlo approach, described in Bauer et al. [5].

Extensions of traditional transfer entropy have been developed. For example, Duan et al. [11] demonstrates the use of direct transfer entropy for root cause analysis, where the transfer entropy is conditioned on other variables in the system.

Duan et al [12] developed transfer 0-entropy, where a distribution is not estimated using KDE. Instead, when the variable has a known range, its uncertainty can be quantified by the Lebesgue measure of the support of this random variable [24].

Rashidi et al. [25] developed a modification of transfer entropy, the symbolic dynamic-based normalised transfer entropy (SDNTE), to address the computational burden of transfer entropy. The developed SDNTE is based on principles of time-series symbolization, xD-Markov machine, and Shannon entropy.

These extensions of transfer entropy can improve the causal analysis, but in many cases they add further complexity to the calculation procedure. For example, application of the direct transfer entropy requires selection of additional embedding parameters. The purpose of this paper is to make causal analysis more accessible for industry practitioners. Therefore the simplest implementation of transfer entropy was chosen.

B. Granger causality

Granger causality is a regression-based interpretation of Wiener's causality definition [22]. Consider the time series of two variables, $\mathbf{x}_i(t)$ and $\mathbf{x}_j(t)$. $\mathbf{x}_j(t)$ can be modelled as an autoregressive (AR) model [26,], as shown in Equation 3, referred to as the *restricted* model.

$$\mathbf{x}_j(t) = \sum_{r=1}^{k} B_j x_j(t-r) + \varepsilon_j(t) \quad (3)$$

In this case only past values of x_j are incorporated to predict future values of itself. In Equation 3: k is the model order defining the time lag; B is the AR coefficient; and ε_j is the prediction error. $\mathbf{x}_j(t)$ can also be modelled incorporating past values of both $\mathbf{x}_i(t)$ and $\mathbf{x}_j(t)$, known as the *full* model as shown in Equation 4.

$$\mathbf{x}_j(t) = \sum_{r=1}^{k} [A_{ji,r} x_i(t-r) + A_{jj,r} x_j(t-r)] + \varepsilon_{j|i}(t) \quad (4)$$

In Equation 4: A_{ji} and A_{jj} represent the regression coefficients. A_{ji}, A_{jj} and B_j can be determined using the least squares approach [27]. The model order, k, can be determined using the Akaike Information Criterion (AIC) [28,]. When the variance of $\varepsilon_{j|i}(t)$ is less than the variance of $\varepsilon_j(t)$, it implies that the prediction of Y is improved by including past values of x_i. x_i is then said to Granger cause x_j [29,]. The Granger causality can be quantified as shown in Equation 5.

$$F_{x_i \to x_j} = \ln \frac{var(\varepsilon_j)}{var(\varepsilon_{j|i})} \quad (5)$$

When the prediction of x_j is not improved by including x_i, $var(\varepsilon_{j|i}(t)) = var(\varepsilon(t))$ and $F_{x_i \to x_j} = 0$. When the prediction of x_j is improved by including x_i, $var(\varepsilon_{i|j}(t)) < var(\varepsilon_i(t))$ and $F_{x_i \to x_j} > 0$ [29,].

For Granger causality, the hypothesis test for significance can take the form of an F-statistical test [29].

Extensions of traditional Granger causality have been developed. For example, Yuan and Qin [15] applied a multivariate extension of Granger causality, where the Granger causality between two variables is conditioned on other variables in the system.

Yuan and Qin, and Landman et al., [14] both applied a frequency domain adaptation of Granger causality (spectral Granger causality) for root cause analysis of oscillations in chemical processes.

Chen et al. [30] incorporated Gaussian process regression into the multivariate Granger causality approach to address

significantly nonstationary or nonlinear variables. Li et al. [31] used a dynamic time warping based method for nonstationary processes

As discussed with transfer entropy, extensions to traditional Granger causality can improve the causal analysis. However, these extensions add complexity to the calculation procedure The purpose of this paper is to make causal analysis more accessible for industry practitioners. Therefore the simplest implementation of Granger causality was chosen.

C. Use of causal maps for fault diagnosis

The goal of the causality analysis is to trace a fault that has propagated through a process to its root cause. Transfer entropy or Granger causality can be calculated between every pair of variables under consideration. Significance testing is then used to remove all connections that fail the significance test. This can be used to construct an adjacency matrix, which is a square matrix whose rows and columns represent process variables, and binary entries represent the edges. An example of an adjacency matrix is presented here:

$$\mathbf{A} = \begin{array}{c|cccc} & LI1 & LI2 & FI1 & TI1 \\ \hline LI1 & 0 & 1 & 0 & 0 \\ LI2 & 0 & 0 & 1 & 0 \\ FI1 & 0 & 0 & 0 & 0 \\ TI1 & 0 & 0 & 1 & 0 \end{array} \tag{6}$$

An entry of 1 in row i, column j, indicates that the node represented by row i has a causal influence on the node represented by column j. An entry of 0 indicates no connection exists. By convention the row represents the *source* element, and the column represents the *sink* element. A causal map can then be constructed from this adjacency matrix. Figure 1 shows the causal map constructed from the adjacency matrix. In this map, nodes represent measured variables in the process, and edges represent significant causal connections between them. This causal map provides a visual representation of the causal structure of the process that can be interpreted to provide information about the root cause of the fault.

The *digraph* function in MATLAB can be used to construct causal maps, and this function has different layout methods to aid visual interpretation. A 'layered' layout reveals such a hierarchical structure [32]. In this layout algorithm the nodes are arranged in a set of layers, so that each edge joins two nodes belonging to different layers. This allows the the sequence of nodes on the propagation path may be visualised in sequential order. In this way, root cause nodes will appear at the top of a graph.

Thicker edges can be used to represent connections with larger Granger causality or transfer entropy values. This may give an indication of which connections are most important in the causal map and may give a clear visual suggestion of the propagation path. The nodes can also be coloured according to their location in the plant. This can either be according to plant sections, units, or even specific controllers, depending on the resolution of interest for the analysis.

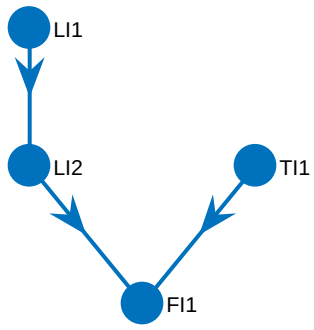

Fig. 1. Example of causal map of adjacency matrix in Equation 6.

III. Comparing the features of Granger causality and transfer entropy

Deciding between the numerous causality analysis approaches can be difficult. Different literature sources may advocate different techniques. Each technique has its own strengths and weaknesses, without clear guidelines for when they are appropriate. The characteristics for which the two techniques are compared are: accuracy, precision, automatability, interpretability, computational complexity, and applicability for different process characteristics.

A. Accuracy and precision of causality analysis techniques

Causality analysis is considered accurate when the method was able to identify the correct root cause of the fault. The method can be deemed useful if the corrective action suggested by the root cause analysis successfully removes the fault.

Uncertainty in process measurements means that non-zero transfer entropy and Granger causality values will be calculated even when there is no causal relationship. As mentioned in Sections II-A and II-B, a hypothesis test is needed to determine the statistical significance of the values. However, this significance test is not infallible, and spurious connections may still be found. These spurious connections make analysis of fault propagation paths difficult. Spurious connections give a false representation of the propagation path of the fault. The reverse is also true, real causal connections might be missed because of this uncertainty.

The validity of individual causal connections can be scrutinised to evaluate the method's accuracy. Spurious and missing connections may also occur due to the limiting assumptions discussed in Section III-E. For example, if Granger causality was used to calculate causality in a process with nonlinear behaviour, the linear regression model may not be able to capture the nonlinear process dynamics and the causal connection may be missed. Non-stationarity in the time series could cause spurious connections for both techniques.

When the ground truth causality is known, one can quantify the missed connection rate, true connection rate, and the false connection rate. Accuracy is defined by high true connection rates and low false and missed connection rates. Precision can be defined by how consistently the method finds the connections.

Section IV evaluates the accuracy and precision of Granger causality and transfer entropy by testing them on a simulated system.

B. Automatability of causality analysis techniques

Application of causality analysis techniques is complex, with numerous parameters to select. The more automated the application procedure is, the less ambiguity there will be in the results. Reduced ambiguity will inspire confidence that the results of the causality analysis reflect the behaviour of the process.

Granger causality is an easily automatable technique. The model order, k, in Equation 5, and the α value for the F-test are the only hyper-parameters to select. The optimal k can be selected as the one that minimises the Akaike information criteria (AIC) [29].

Parameter selection for transfer entropy is more complicated. Equation 1 shows that four parameters need to be selected, K, L, H, and τ. The transfer entropy results are sensitive to these parameters [3], [33]. Parameter search procedures are typically employed [9], [11], but are computationally expensive and therefore difficult to implement. Many researchers use the default parameters suggested by Bauer et al. [5]. In previous work, the authors of this paper [33] presented a systematic, automated workflow for application of transfer entropy for oscillation diagnosis. This workflow presents guidelines for calculation parameter selection based on process dynamics, namely the time delay between variables and the oscillation frequency. Additionally, clear guidelines were given for each step in the application procedure. This systematic workflow can also be modified to replace transfer entropy with Granger causality. Therefore both Granger causality and transfer entropy can be automated easily with this workflow.

C. Interpretability of causality analysis techniques

Fault diagnosis techniques are used by engineers to gain insight into abnormal behaviour occurring within a process. The engineer has to interpret the causal map to see whether a clear propagation path is manifested. It is important that the engineer can understand the information presented simply, and understand the implications. For example, when a spurious connection passes the significance test because of excessive noise in the signal, and is displayed on the causal map, the engineer will need to use process knowledge and understanding of the causal statistic to understand why that spurious connection was found.

This interpretation has two components: mathematical interpretation of the underlying causal statistic; and visual interpretation of the causality maps.

1) Mathematical interpretation: For both Granger causality and transfer entropy, the causal statistics are not directly linked to any physical engineering quantity. However, it is easier to reason about the Granger causality since it is based on simple regression statistics. The significance test, the F-test, is also based on a known distribution. The information theory used for transfer entropy is more complicated, and interpretation of the values obtained is not straightforward. Furthermore, the significance test based on Monte Carlo simulations used for transfer entropy is more difficult to interpret than that based on a known distribution used for Granger causality.

2) Visual interpretation: The end result of the causality analysis is a causality map. When this causality map gives a clear indication of the propagation path that is logically consistent with process knowledge, then the variables at the start of the propagation path can be further investigated. When the suggested propagation path is ambiguous it may be uncertain what the root cause was. There may be more than one suggested propagation path in the causal map pointing to different root cause variables. In the case where these different root cause variables are associated with the same unit in the plant, or the same controller, then it can be inferred that the root cause is closely associated with that unit and can be investigated. When there are multiple root causes all associated with different units, or sections of the plant, then the root cause is more ambiguous. In this scenario it is possible that multiple faults are occurring simultaneously [34]. However, a simplifying assumption that only one fault occurs at any time is applied, since the probability of occurrence of simultaneous independent faults is small, as suggested by Shiozaki et al. [35]. A more likely scenario is that the numerous root nodes identified are manifestations of the same fault that simultaneously affected different measured variables.

All causal effects in a system are identifiable when the causal map is acyclic [36]. Cyclical causal maps, where each node is reachable from any other node [37], show no clear start or end nodes, and therefore give no clear indication of where to further investigate the fault.

Because this interpretation is complicated, the decision flow presented in Section V provides steps for dealing with ambiguous root causes.

The visual interpretability of the causality maps for either Granger causality or transfer entropy will be a function of the accuracy of the method. Large amounts of spurious connections will make it difficult to interpret the causal map. The visual interpretability will also be affected by the complexity of the system which the causal map represents. However, visualisation tools described in Section II-C can be applied to the causality maps from either technique to aid with visual interpretation.

D. Computational complexity of causality analysis

Transfer entropy is a computationally expensive technique. Duan et al. [38] derived the computational complexity for transfer entropy as $O(N^2(K+L)^2)$, where K and L represent the embedding dimensions chosen, and N represents the number of samples. Lindner et al. [33] suggested values were $K = 1$ and $L = 2$ to limit the computational complexity. These calculations are repeated when the significance calculations are performed. In a previous work the authors of this paper suggested 100 surrogate repetitions [33].

For Granger causality the core calculation is the least squares regression of the $N \times Mk$ matrix, where k is the model order, N is the number of samples, and M is the

number of variables. This distils to a $O(M^3k^3N)$ problem for a specific model order, k. This is repeated for a range of model orders that cover the time spans common in processes. For most chemical and mineral processes, the unit residence times are at most of the order of a few minutes [39]. Therefore, at a sampling time of around 10s, which is common for data historians, the range of model orders is typically from $k = 1 : 30$. The typical values for M depend on the size of the plant being monitored and the problem being analysed. However, typical values are between 10 and 30 variables. The typical values for N range from a minimum of 500 samples [5], [33], to arbitrarily large numbers of samples. However, around 2000 samples is common.

To generalise the computational time required to perform the significance threshold calculations for transfer entropy, the time taken for a single pair of variables was calculated while varying the number of samples. The computational time as a function of the number of samples could then be obtained. It must be noted that it was not attempted to optimise the transfer entropy code used for this analysis, apart from the use of parallel computation. More mature toolboxes for transfer entropy, such as JIDT [40], may provide faster computation time.

Figure 2 shows the computational time required to calculate the significance threshold for a single pair of variables, for 100 surrogates, as a function of the number of samples. The computational time was found to be a power law function of the number of samples, $CPU_{time} = 34 \times N^{0.5}$. The relative transfer entropy method method was used (Equation 2), which is symmetrical, and self pairs are ignored, so this has to be repeated $(M^2 - M)/2$ times. The calculation of the PDFs is a very parallel problem, and therefore it can be assumed that doubling the amount of cores halves the computational time. This is a simplifying assumption that ignores some of the inefficiencies that are introduced by splitting iterations among parallel workers. Therefore, a rough estimate of the amount of time taken for the calculation of transfer entropy is given by Equation 7.

$$CPU_{time} = \frac{34 \times N^{0.5}(M^2 - M) \times N_{cores}}{2} \tag{7}$$

The computational complexity for transfer entropy is higher than that for Granger causality. The decision flow in Section V therefore incorporates a preliminary complexity analysis, to decide whether the time it will take to compute transfer entropy is excessive or not. What amount of time is considered excessive depends on the situation. Online, automated fault diagnosis would require a solution within minutes. If the plant is experiencing an ongoing fault the engineer needs to isolate the root cause as fast as possible to return the plant to normal operation. On the other hand, if the analysis is being performed offline to gain more information about fault conditions that happened some time in the past, the engineer may not mind waiting a few hours for results.

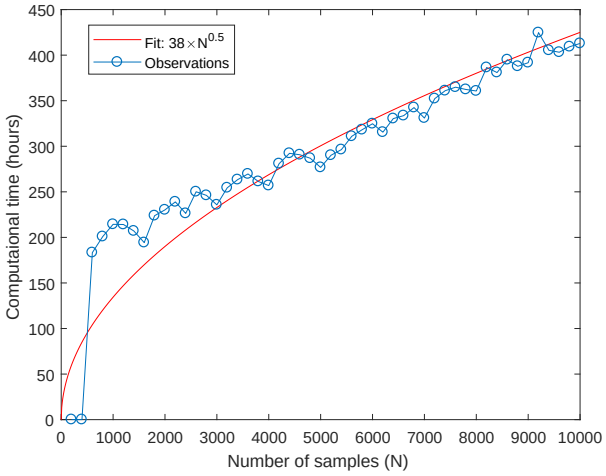

Fig. 2. Computational time required to calculate transfer entropy significance for one pair of variables as a function of number of samples. System used: 32 GB RAM, 3.33 GHz processor. The computational time was found to be well approximated by $CPU_{time} = 34 \times N^{0.5}$

E. Applicability for different process characteristics

The applicability of a causality analysis technique may be limited by the underlying assumptions of the calculations it is based on.

Traditional Granger causality incorporates linear regression, and may therefore be limited in its ability to capture nonlinear behaviour in time series trends. Transfer entropy is not limited by this linear model assumption. Many chemical and mineral processes are known to contain nonlinear interactions. Applying a nonlinearity identification technique may help decide whether Granger causality or transfer entropy is appropriate for the system under consideration. However, nonlinear systems often behave linearly over large-scale interactions [29]. Nonlinear adaptations of Granger causality have been developed [29]. For example, Marinazzo et al. [41] developed a kernel-based extension of Granger causality.

In industrial processes, control systems maintain process variables close to a desired operating region where the system behaviour typically remains linear. The fault affecting the process may have originated from nonlinear phenomena, such as valve stiction. In such cases the process acts as a mechanical low pass filter as the oscillation propagates to different variables [42]. The low-pass process dynamics remove the higher harmonics in the trends and destroy phase-coupling. This means that nonlinear behaviour is unlikely to be sustained in the process.

Although transfer entropy is not limited to linear systems, the joint PDFs need to be calculated for stationary time series. This means that the autocorrelation, mean, and variance of the time series are not a function of time [43]. Granger causality also assumes stationarity to calculate the regression coefficients. Extensions to Granger causality have been proposed to address nonstationary and nonlinear time series. Chen et al. [30] incorporated Gaussian process regression into the multivariate Granger causality approach to address significantly nonstationary or nonlinear variables. Li et al.

used a dynamic time warping based method for nonstationary processes

Kühnert [19] presented guidelines for technique selection based on process characteristics. These guidelines were developed based on simulated experiments to determine which technique gave the most accurate results for different process characteristics. They found that transfer entropy was applicable for both linear and nonlinear systems, and applicable for systems with long dead time and short dead time between variables. They also found that Granger causality was only applicable for linear systems with short dead time between variables.

This indicates that transfer entropy is more generally applicable than Granger causality.

IV. Comparing the accuracy and precision of Granger causality and transfer entropy in a simulated system

To compare the accuracy and precision of Granger causality and transfer entropy, their ability to find true connections in a simulated process was tested. The causal maps obtained from Granger causality and transfer entropy were compared to the true causal map to classify edges as true connections, false connections, or indirect connections. Since the simulation added random noise to the signals, repeated measurements could be taken. The repeated measurements allowed the precision of each technique to be evaluated.

A. Description of simulated process case study

A simple process of two tanks in series with heat exchangers was simulated. Figure 3 shows a diagram of the process. The tank levels are controlled by the flow of cold water into the tanks using PID controllers. The tank temperatures are controlled by the steam flow rate through the heating coils using PID controllers. Random noise was added to the signals to simulate noise in the process.

An oscillation was introduced in the cold water input temperature, $T1in$. Figure 4 shows the oscillations in the signals from one of the repeated simulations. This oscillation would propagate through the process from $T1in$ by first affecting the first tank's temperature $T1$. The temperature controller would then change the steam flow rate, $F3$, to compensate. The controller is unable to fully reject the input disturbance, the second tank's temperature, $T2$, would also be affected. The second tank's temperature controller would then change the steam flow rate, $F4$, to compensate. The actual propagation path of the oscillation is known, and can therefore be used as ground truth to compare the causal maps obtained from Granger causality and transfer entropy. This true propagation path is shown in Figure 6a.

This simulation was repeated 1000 times. Only the random noise added to the signals was altered between simulations, so the oscillation affecting the process remained the same.

B. Comparison of Granger causality and transfer entropy to ground truth in simulated case study

Granger causality and transfer entropy were used to analyse the signals from the two tank simulation to identify the

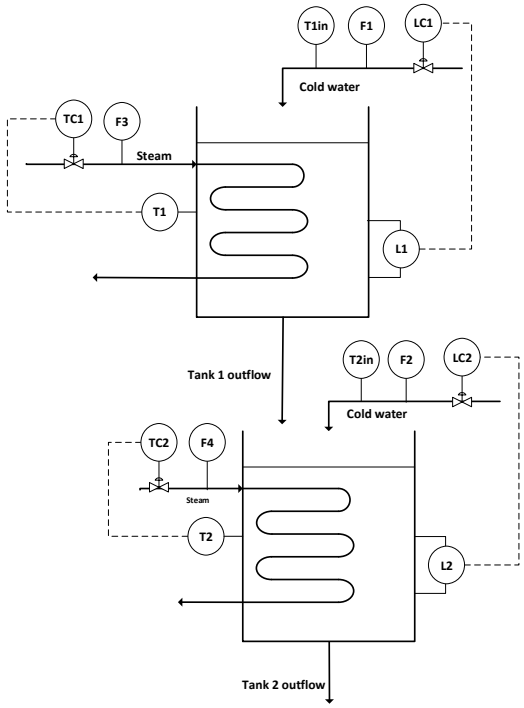

Fig. 3. Diagram of simulated two tank process. Two tanks in series with heat exchangers. Tank levels are controlled by the flow of cold water into the tanks, tank temperatures are controlled by the steam flow rate through the heating coils. Random noise was added to the signals.

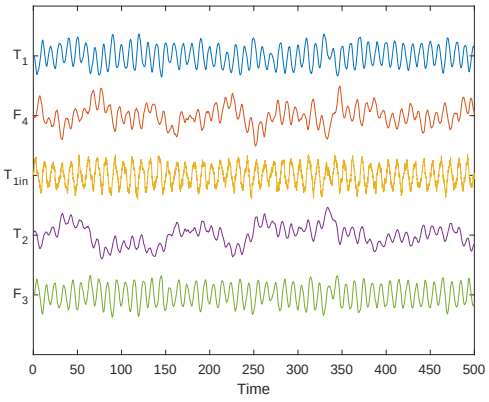

Fig. 4. Oscillations in signals in two tank process.

propagation path of the oscillation. The resulting causality maps were compared to the true propagation path derived from first principles knowledge of the process, shown in Figure 6a. The edges in the causality maps were classified as true connections, false connections, or indirect connections. Indirect connections are defined when a causal connection is identified due to the influence of an intermediate variable. Accuracy metrics are defined as follows:

Definition 1: True connection rate (TCR): the fraction of causal connections in the true propagation path that were

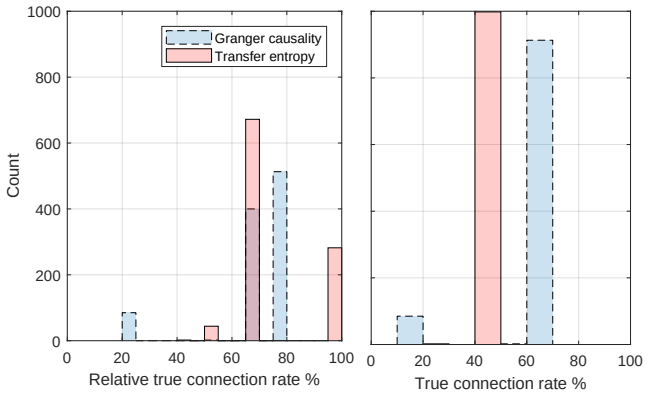

Fig. 5. Distributions of true connection rates and relative true connection rates for Granger causality and transfer entropy in the simulated two-tank process.

detected using the data-based technique:

$$TCR = \frac{C_{detected,true}}{C_{knowledge}} \tag{8}$$

where $C_{detected,true}$ is the number of true causal connections found using the data-based technique, and $C_knowledge$ is the number of connections in the true propagation path. This is the opposite of the missing connection rate (MCR): $MCR = 1 - TCR$.

Definition 2: Relative true connection rate (RTCR): the fraction of total edges in the causality map that are true connections:

$$RCTC = \frac{C_{detetcted,true}}{C_{detected}} \tag{9}$$

where $C_{detected,true}$ is the number of true causal connections found, and $C_{detected}$ is the total number of detected connections. This is the opposite of the relative false connection rate (FCR): $FCR = 1 - RTCR$.

TABLE I
MEANS AND STANDARD DEVIATIONS OF TRUE CONNECTION RATES AND RELATIVE TRUE CONNECTION RATES SHOWN IN FIGURE 5.

	Transfer entropy	Granger causality
TCR Mean	50%	62%
TCR Standard deviation	1%	14%
RTCR Mean	75%	70%
RTCR Standard deviation	16%	16%

Figure 5 plots the distributions of the true connection rate and relative true connection rate for both Granger causality and transfer entropy for the 1000 repetitions. Table I shows the means and standard deviations obtained.

The means of the distributions indicate accuracy. Transfer entropy showed a higher mean RTCR, but a lower mean TCR. This indicates that although it doesn't find all the true connections, the connections that it does find are more likely to be true connections. The variance of the distributions give an indication of precision. The standard deviation for transfer entropy is very low for the TCR, and the standard deviations for the two techniques are almost identical for the RTCR. This indicates that transfer entropy is more precise than Granger causality.

Representative samples of the Granger causality and transfer entropy results are presented along with the true propagation path in Figure 6.

Granger causality consistently found strong connections related to the control connections between F_3 and T_1, and F_4 and T_2. In these control loops, T_1 and T_2 are the controlled variables (CV), and F_3 and F_4 are the manipulated variables (MV). This is because the introduction of the oscillation to the process causes excessive controller action, strengthening the causal relationship between its CV and MV. Transfer entropy also consistently found the control connection from F_4 to T_2. Transfer entropy consistently found the connection from $T_{1,in}$ to T_1. This connection shows the propagation from the input temperature.

Granger causality found indirect connections often. This means that some of the low RTCRs observed in Figure 5 are actually because indirect connections were not taken into account. For this system, transfer entropy did not find any indirect connections. Indirect connections may be considered to be misleading. Identifying all the direct connections along the propagation path of the oscillation will give insight into the symptoms and the root cause of the oscillation. However, indirect connections still provide this information at lower resolution, missing some connections along the way.

C. Summary of simulated case study comparing Granger causality and transfer entropy

Considering the relative true connection rates, transfer entropy was slightly more accurate. The standard deviations also indicated that transfer entropy was more precise. These results must be considered with caution. Simulated systems are useful for constructing controlled experiments and repeated experiments, but they can never fully replicate the common cause variation and complex interactions in real processes.

V. DECISION FLOW FOR APPLICATION OF GRANGER CAUSALITY OR TRANSFER ENTROPY

Section III compared the features of Granger causality and transfer entropy. Section IV then compared their accuracy and precision using simulated experiments. A decision flow was developed to aid users in deciding when to use Granger causality or transfer entropy, as well as to aid in the interpretation of the causality maps obtained from these techniques. This decision flow was developed from the comparisons in Sections III and IV, as well as from the experience of the authors using causality analysis for fault diagnosis. This decision flow is presented in Figure 7.

The first step is to perform a computational complexity analysis that takes into account the number of samples, the number of variables, and the computational resources available. Equation 7 can be used to estimate the calculation time required for transfer entropy. If the calculation time is acceptable, transfer entropy is preferred, since it has been found to be more accurate and precise and yields more visually interpretable causality maps, as demonstrated in Section VI. If the calculation time is unacceptably large, then Granger causality can be used. Granger causality analysis can be

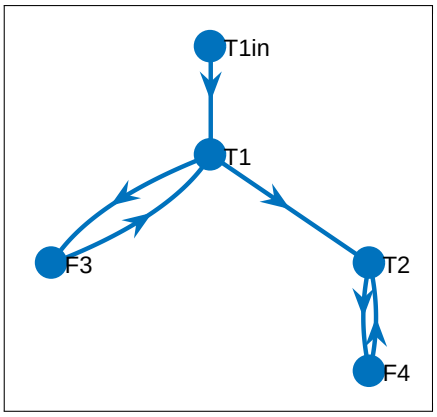

(a) True propagation path

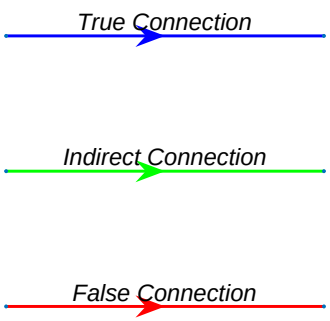

(b) Legend

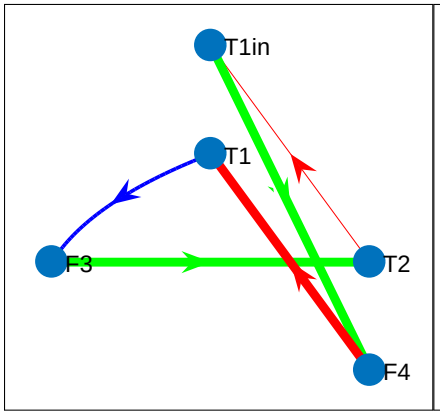

(c) Granger causality minimum

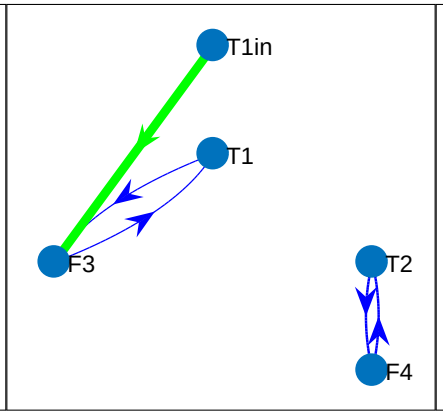

(d) Granger causality median

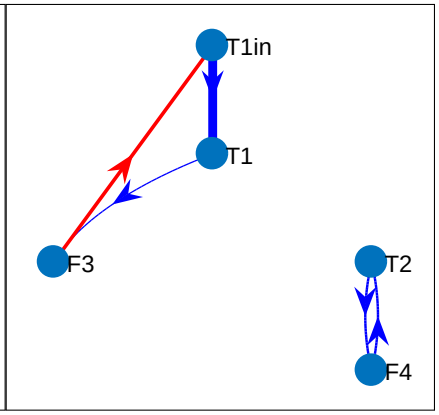

(e) Granger causality maximum

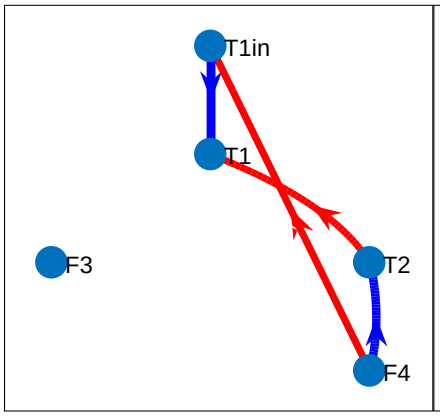

(f) Transfer entropy minimum

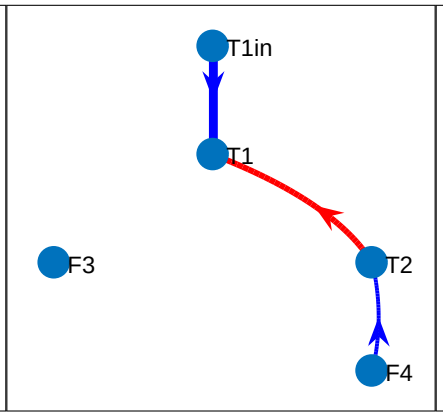

(g) Transfer entropy median

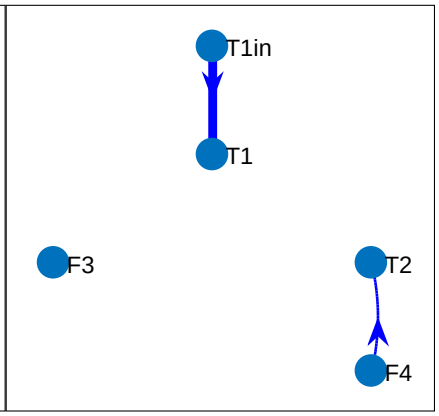

(h) Transfer entropy maximum

Fig. 6. Granger causality and transfer entropy results from repeated simulated experiments compared to true propagation path. Results shown from minimum, median, and maximum true connection rates.

performed and the accuracy can be evaluated from process knowledge. If numerous spurious connections are observed then transfer entropy can be employed instead, since transfer entropy is more accurate. If not, the propagation path can be interpreted.

The authors' previous experience [13], [33], [44]–[48] has shown that interpretation of causal maps is complicated. The interpretation of the propagation path starts with determining whether the causal map is acyclic. An acyclic map has a definitive start node and end nodes, giving a clear suggestion of the sequence of nodes in the propagation path. When a cyclical map shows stronger connections for some of the edges it may still indicate important connections along the propagation path. When an acyclic map shows a single root node, this gives one possible root node that can be investigated further. Sometimes an acyclic map shows multiple root nodes. However, if all these nodes are localised to the same unit in the plant, or possibly to the same controller, this part of the plant can be investigated further. If there are multiple root nodes that are not related to a specific unit or controller in the

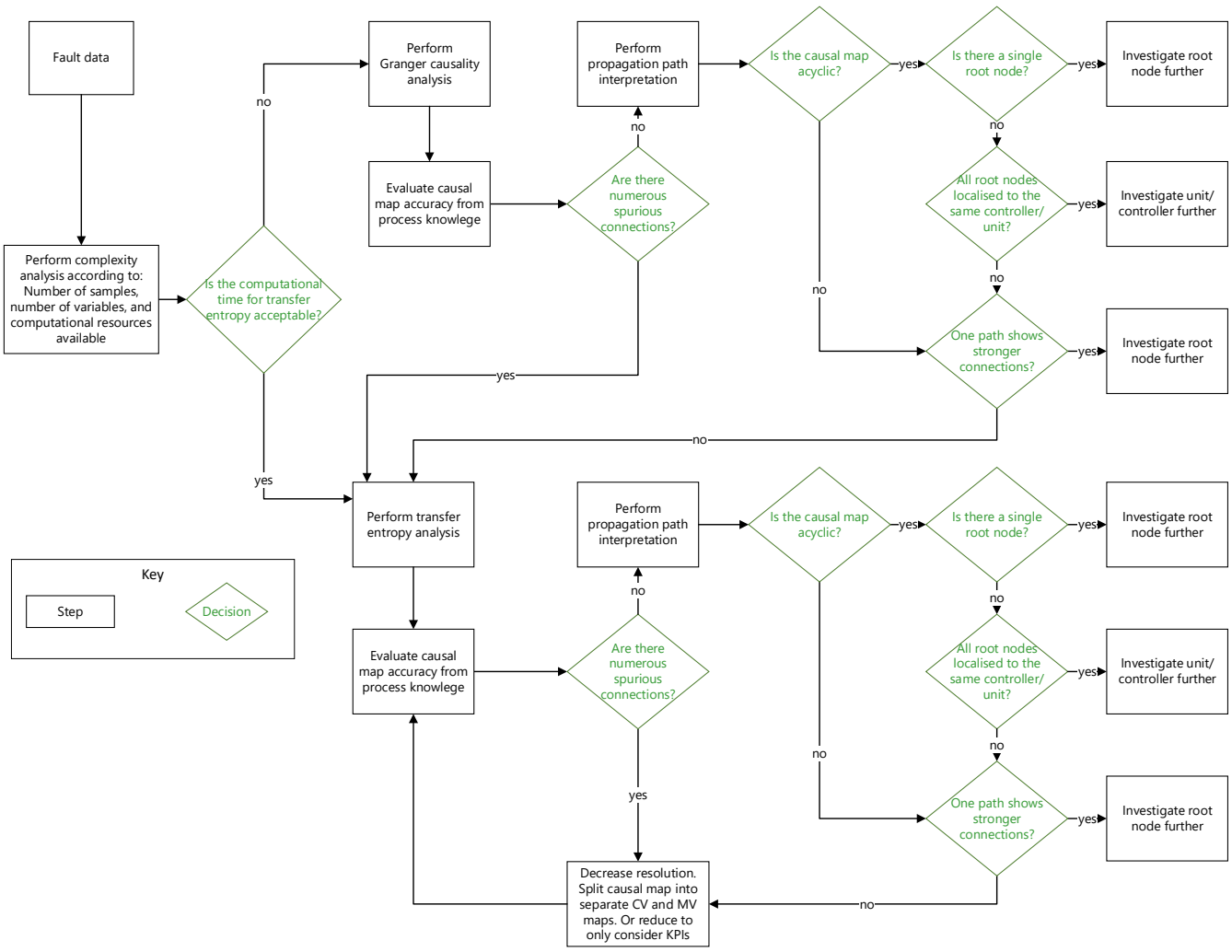

Fig. 7. Decision flow for application of Granger causality or transfer entropy for fault diagnosis.

plant, the strength of the connections may give an indication of which of the root nodes is most important. This node can then be investigated further.

If no definitive root cause is obtained from following the propagation path interpretation decision flow, then transfer entropy can be applied.

The same procedure is followed after performing the transfer entropy analysis. The causal map accuracy is evaluated from process knowledge. If numerous spurious connections are found, this time the resolution of the causal map can be decreased. This can be achieved separating the causal map into smaller groups of variables. For example, the map can be split to just contain controlled variables, or manipulated variables. In previous work this separation was applied and found to be effective [13]. By reducing the resolution, the density of the graph, the number of edges per node, may be reduced and a propagation path may be more visible. After resolution reduction the evaluation can be performed again. If there are not numerous spurious connections, the propagation path interpretation can be performed. If no definitive root cause is obtained from following the propagation path interpretation decision flow, then the resolution reduction can be performed again.

VI. Illustrating the features of Granger causality and transfer entropy on an industrial case study

To illustrate the features of Granger causality and transfer entropy discussed in Section III, as well as to demonstrate the decision flow presented in Section V, both techniques were used to analyse a plant wide oscillation in a mineral concentrator plant.

A. Case study description

A simplified flow diagram of the industrial process is shown in Figure 8. Previous work by the authors of this paper [13] investigated an oscillation in a part of the same process. In the primary milling section, ore rocks are ground up to liberate the valuable minerals from the gangue (non-valuable) mineral. The ground up fines are sent to a sump, which is a surge tank where water is added to control the level. The slurry is then sent to a hydrocyclone for separation. Oversized

particles are recycled to the mill, while fine particles are sent to the flotation section. Flotation is used to separate the valuable and gangue particles, by selectively imposing hydrophobicity on the valuable mineral particles. This causes the valuable particles to attach to air bubbles and float to the top of the cell [39]. The final tails are combined and sent to the secondary milling circuit. The secondary milling circuit operates similarly to the primary milling circuit.

Oscillations were observed in the mass pull of the flotation circuit, which is an important key performance indicator (KPI), and is included in the advanced process control (APC) strategy of the flotation circuit. The mass pull is the proportion of the feed material reporting to the concentrate [39]. The oscillation persisted for 12h35min. The period of the oscillation in the mass pull signal was 69 min.

The root cause of the oscillation was uncertain from first inspection, because the variables used to control the mass pull, namely the flotation cell levels and the air addition to the cells, did not show abnormal trends. However, by analysing the frequency spectrum to find the peak oscillation frequencies, it was observed that 27 of the monitored variables displayed this shared oscillation frequency (see Appendix A). The time series trends of these variables are plotted in Figure 9. These variables are spread throughout three sections of the plant: the primary milling section; the flotation section; and the secondary milling section. Since the Primary Mill circuit is the first processing unit in the plant, it appears that the oscillation originated within that circuit. However, since the milling circuit contains a recycle stream, it is not apparent from first inspection which unit or controller was associated with the start off the oscillation. This makes it a useful case study for testing causality analysis techniques.

The workflow presented in [33] was followed to analyse this oscillation. This paper does not focus on the application procedure, but Appendix A presents the details.

B. Transfer entropy results

The causal map obtained from transfer entropy is shown in Figure 10.

Following the decision flow in Figure 7, the first step after performing transfer entropy is to evaluate the accuracy of the causal map by identifying whether there are spurious causal connections. This step requires knowledge of the process. To augment the causal map with process knowledge, the nodes in the causal map have been coloured according to which section of the plant they are located in. Blue indicates primary milling section, green indicates the flotation section, and yellow indicates the secondary milling section. The overall material flow of the plant, as shown in Figure 8, is from primary milling to flotation to secondary milling. The causal map should generally reflect this flow, showing nodes going from blue to green to yellow, and not in the opposite direction.

In the causal map shown in Figure 10, the only spurious connection is the causal connection from Cell 3's velocity ($FT3Velocity$) to Sump 1's outflow ($SU1OutflowMV$). The flotation cell, Cell 3, is downstream of Sump 1 in the process, and no controller interaction could account for this connection. This spurious connection is not on the propagation path from the other root nodes, Sump 1's water addition setpoint ($SU1WaterSP$) and Sump 1's level ($SU1LevelPV$). Therefore the spurious connection can be ignored without influencing the interpretation of the causal map.

The next step in the decision flow is to interpret the propagation paths in the causal map. The first question is, 'Is the graph acyclic?'. In this case the graph is acyclic, with visible start nodes, Sump 1's water addition setpoint ($SU1WaterSP$) and Sump 1's level ($SU1LevelPV$), and end node Sump 5's density ($SU5Density$). There is a cyclical section of the graph, between Sump 1's water addition MV ($SU1WaterMV$), Sump 1's outflow setpoint ($SU1OutflowSP$), and Sump 1's density ($DensitySU1$). However, this cycle does not interfere with the main propagation path between the root nodes Sump 1's water addition setpoint ($SU1WaterSP$) and Sump 1's level ($SU1LevelPV$) and the end node Sump 5's density ($SU5Density$).

The next question in the workflow is, 'Is there a single root cause variable?' The answer is no. The causal map suggests three possible root cause variables: Sump 1's water addition setpoint ($SU1WaterSP$), Cell 3's velocity ($FT3Velocity$), and Sump 1's level ($SU1LevelPV$). As described earlier, the connection from Cell 3's velocity to Sump 1's outflow is a spurious connection, and can be excluded from further analysis. This leaves two root cause variables. The next question is, 'Are all the root nodes localised to the same controller/unit?' Sump 1's water addition setpoint ($SU1WaterSP$) and Sump 1's level ($SU1LevelPV$) are both associated with Sump 1's level controller. So the answer is yes. The decision flow suggests that Sump 1's variables should be investigate further as possible root cause variables.

Figure 11 shows the time series trends of the sump variables at the start of the oscillation. The trends indicate that the sudden drop in the sump level occurred first. This caused the sump level controller to compensate by varying the sump feed water. This sump water fluctuation resulted in fluctuations in the sump density. This density variation propagated through the flotation circuit to the secondary milling circuit. The causal map confirms this, showing Sump 5's density ($SU5Density$) to be the end node. The variation in density throughout the flotation circuit had a severe impact on flotation performance, since the hydrodynamic properties of the contents of the flotation cells had changed. This is what caused the mass pull to oscillate, even though most of the cell levels remained normal. The flotation circuit is equipped with a multivariable level control strategy. This means that the level oscillation in the sump was effectively rejected in the flotation section, and the cell levels did not oscillate. The cause of the oscillation in the mass pull was therefore not clear. This illustrates the need for a causal analysis tool such as transfer entropy to investigate such events.

In addition to the propagation paths from the primary milling section through to the secondary milling section, the direct causal connection from Sump 1's level to Bank 2's mass pull ($SU1LevelPV \rightarrow MasspullB2$) indicates that the oscillations in the sump level strongly contributed to the oscillations in the mass pull. This direct connection may

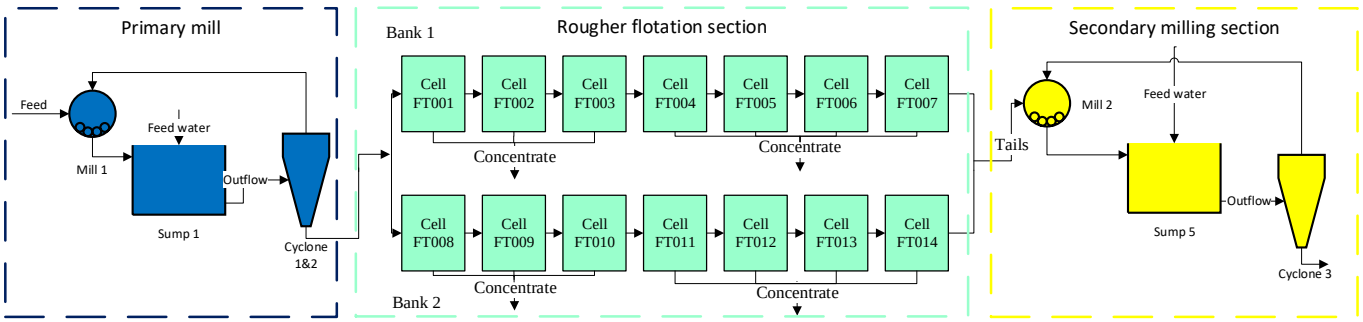

Fig. 8. Simplified process flow diagram showing the primary milling circuit, the rougher flotation section and the secondary milling section.

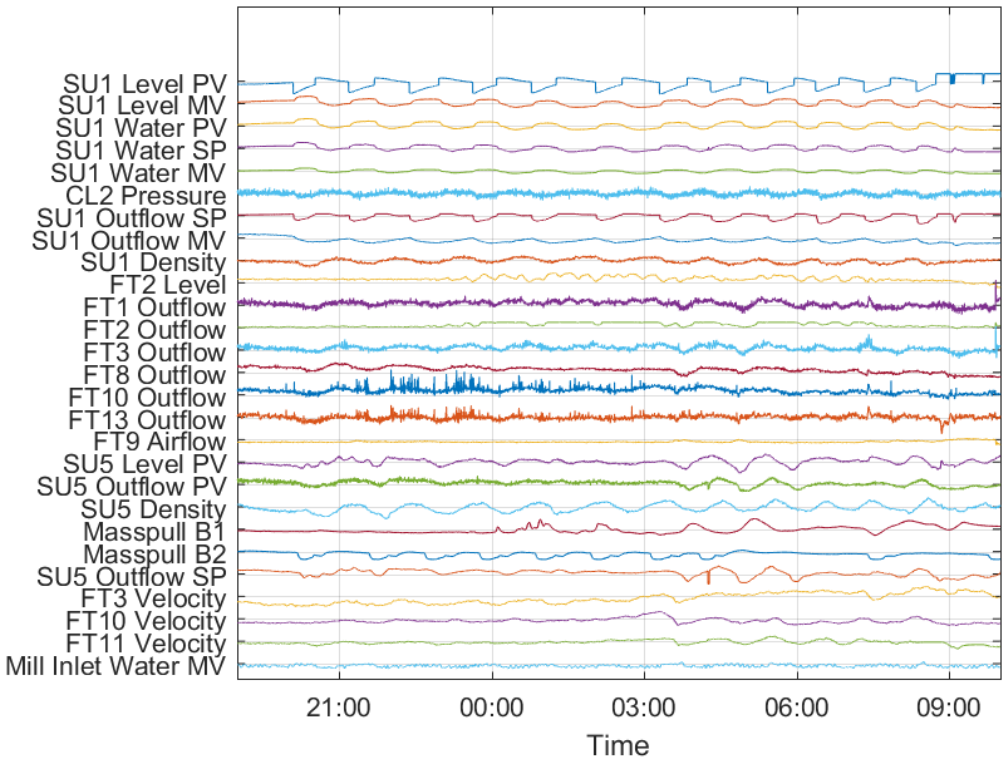

Fig. 9. Trends for all variables showing oscillation at period of 69 minutes. This includes variables from primary milling circuit, rougher flotation circuit, and secondary milling circuit.

seem misleading, since the actual propagation path would flow through a number of intermediate variables first before affecting the mass pull. However, the direct connection still displays useful information about where the oscillation originated.

Transfer entropy effectively isolated the root cause of a plant-wide oscillation to a single unit. The causal map generated using transfer entropy is a useful visual tool for root cause analysis. The causal map is easily interpretable, showing a clear propagation path with only one spurious connection.

C. Granger causality results

The propagation path obtained for Granger causality is shown in Figure 12. The same workflow used for transfer entropy, described in Appendix A, was used. The only difference in the application was that Granger causality was substituted in for transfer entropy for the causality analysis procedure.

Following the decision flow in Figure 7, the first step after performing Granger causality is to evaluate the accuracy of the causal map by identifying whether there are spurious causal connections. As done with the transfer entropy, the nodes were coloured to reflect the plant section. The cyclical nature of the graph does not reflect the material flow in the process.

In the causal map shown in Figure 12, there are multiple spurious connections. The connection from Sump 5's density to Bank 1's mass pull ($SU5Density \rightarrow MasspullB1$) and Sump 5's outflow setpoint to Cell 3's velocity ($SU5OutflowSP \rightarrow FT3Velocity$) are both spurious since the secondary milling section is downstream of the flotation section, and no material flow or control would

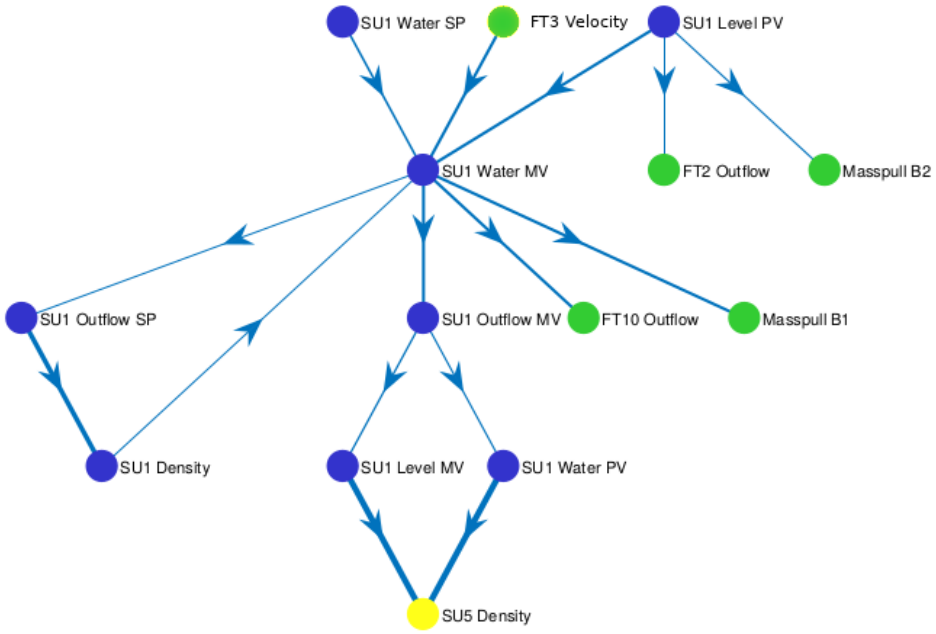

Fig. 10. Transfer entropy propagation paths for oscillations in the primary milling, flotation, and secondary milling circuits. Values displayed on edges and edge width represent the transfer entropy value calculated. Colours on nodes indicated the section of the plant where the variables are located.

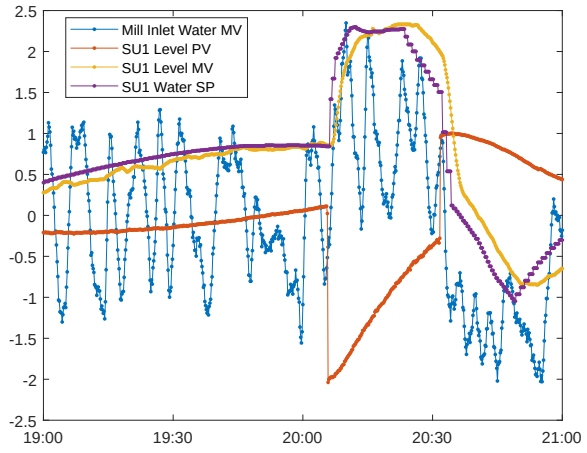

Fig. 11. Time series plots of sump variables at start of oscillation.

create these causal connections. The connection from Cell 11's velocity to Sump 1's level ($FT11Velocity \rightarrow SU1LevelPV$) is spurious, since the flotation section is downstream of the primary milling section. The connection from Cell 3's outflow to Cell 8's outflow ($FT3Outflow \rightarrow FT8Outflow$) may be spurious, since these are variables from two separate flotation banks that could not affect each other. In general the causal map has one main propagation path, and all of these spurious connections are part of that path. This means that these connections cannot be ignored without affecting the interpretation of the propagation path. If the decision flow in Figure 7 were being followed, then the answer to the question 'Are there numerous spurious connections?', would be yes. The decision flow then suggests that the causality analysis be repeated with transfer entropy instead.

Although the decision flow suggests that Granger causality is no longer useful in this scenario, it is still worth examining the causal map to compare the features to the transfer entropy causal map. The next step in the decision flow is to interpret the propagation paths in the causal map. The first question is, 'Is the graph acyclic?'. In this case the graph is cyclic, there is no clear start node or end node. The next question is, 'Does one path show stronger connections?'. In this causal map there is a propagation path from Sump 1's level to Sump 1's outflow setpoint ($SU1LevelPV \rightarrow SU1WaterSP \rightarrow SU1WaterMV \rightarrow SU1OutflowSP$) with strongly weighted connections. This does indicate that Sump 1's level controller is closely associated with the root cause of the oscillation.

Careful interpretation of the causal map revealed the same information that the transfer entropy analysis did. However, because of the numerous spurious connections and the cyclical nature of the causality map the results were much harder to interpret than the transfer entropy results.

D. Summarising the difference between Granger causality and transfer entropy for the industrial case study

Now that both Granger causality and transfer entropy have been tested on the industrial case study, the features discussed in Section III can be compared.

1) Accuracy: Both Granger causality and transfer entropy provided tools to accurately isolate the oscillation to the

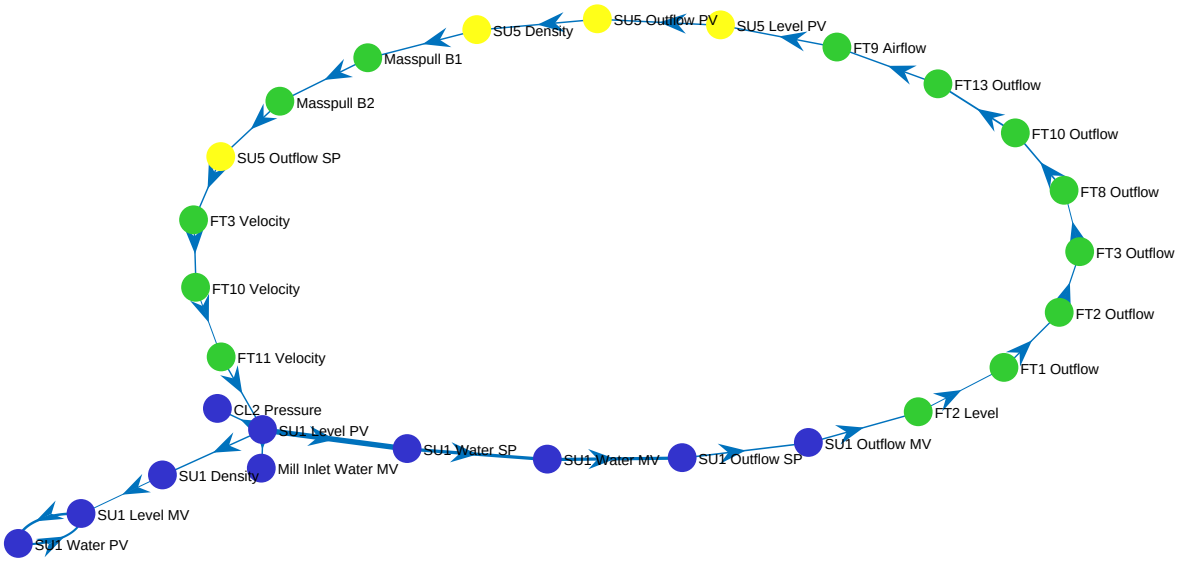

Fig. 12. Granger causality propagation paths for oscillations in the primary milling, flotation, and secondary milling circuits. Values displayed on edges represent the Granger causality value calculated.

primary mill sump. Data-based techniques for root cause analysis are limited to measured variables. This means that both Granger causality and transfer entropy would not be able to point directly to the underlying cause of the fault, but can direct the attention to measured variables closely associated with it.

Granger causality resulted in three causal connections that could be confidently identified as spurious, and one that is probably spurious, based on process knowledge. Transfer entropy resulted in only one spurious connection. Therefore, on the basis of the number of false connections, transfer entropy was more accurate in this case study.

2) Automatability: Using the workflow suggested in a previous work by the authors of this paper [33], the application procedure for transfer entropy and Granger causality were both fully automated.

3) Interpretability: Transfer entropy generated a causal map with a clear propagation path. Two possible root nodes were identified, but since both were related to the same controller the propagation path was still clear. Granger causality resulted in a cyclical causal map with no clear start and end nodes. By examining connection strengths some useful information about the oscillation propagation could be inferred. Therefore transfer entropy gave a more visually interpretable causal map.

4) Computational complexity: The CPU time required for computation of each method was quantified. The computer used was a computational server with 32 GB RAM and 3.33 GHz processor. For transfer entropy, parallel computation was used in the computation of the PDFs, where 8 parallel workers were used. As expected, transfer entropy was much more computationally expensive than Granger causality. Granger causality only took 2.5 minutes. Transfer entropy took 27 hours. This is prohibitively long for rapid analysis of the root cause. Of that time, the transfer entropy calculation itself between all 27 variables only took 15 minutes. The significance testing using Monte Carlo simulations of surrogate time series took the rest of the time.

5) Applicability for different process characteristics: In this case study some of the oscillations, for example in $SU1LevelPV$, showed nonlinear behaviour. This may be why Granger causality showed more spurious connections than transfer entropy. The time series trends of all the variables included in the analysis were stationary for the period under observation, showing no change in the mean or autocorrelation over time.

VII. Chapter Conclusion

This paper presented a comparative analysis of Granger causality and transfer entropy used for fault diagnosis in an industrial process. The comparison was based on the following features: accuracy, precision, automatability, interpretability, computational complexity, and applicability for different process characteristics.

Transfer entropy was found to be more generalisable, and visually interpretable. However, Granger causality was found to be easier to automate, much less computationally expensive, and easier to interpret the meaning of the values obtained. To directly address the the accuracy and precision of Granger causality and transfer entropy, their ability to find true connections in a simulated process was tested. The results indicated that transfer entropy showed higher accuracy and precision.

A decision flow was developed from these comparisons to aid users in deciding when to use Granger causality or transfer entropy, as well as to aid in the interpretation of the causality maps obtained from these techniques. This decision flow is presented in Figure 7.

The features of Granger causality and transfer entropy were illustrated on an industrial case study of oscillations in a mineral processing plant. In this case study, the causal map obtained from the transfer entropy analysis showed two root cause variables associated with the same unit in the process. The transfer entropy results were able to provide useful information for further analysis into the cause of the fault. Granger causality, on the other hand, showed a large number of spurious connections, and gave no clear indication of the root cause.

Future research may focus on more automated graph interpretation strategies. Further augmenting the causality maps with process knowledge may improve this interpretation process. Examining the causal graphs by hand to determine whether spurious connections exist is time consuming and error prone. Spurious connections could be automatically flagged by comparing causal maps to connectivity from plant diagrams.

The computational burden of transfer entropy is still a barrier for potential adoption. The computational time is dominated by the time taken to perform the significance calculations. If this time could be reduced the barrier could be reduced. For example if the surrogate time series for two variables showed similar harmonics they could be used as proxies for each other. Then the amount of surrogate pairs required could be reduced.

REFERENCES

[1] F. Yang, T. Chen, S. L. Shah, and P. Duan, *Capturing Connectivity and Causality in Complex Industrial Processes*, ser. SpringerBriefs in Applied Sciences and Technology. Cham: Springer, 2014.

[2] F. Yang and D. Xiao, "Progress in Root Cause and Fault Propagation Analysis of Large-Scale Industrial Processes," *Journal of Control Science and Engineering*, vol. vol. 2012, pp. Article ID 478 373, 10 pages, 2012.

[3] P. Duan, T. Chen, S. L. Shah, and F. Yang, "Methods for root cause diagnosis of plant-wide oscillations," *AIChE Journal*, vol. 60, no. 6, pp. 2019–2034, Jun. 2014.

[4] M. Reis and G. Gins, "Industrial Process Monitoring in the Big Data/Industry 4.0 Era: from Detection, to Diagnosis, to Prognosis," *Processes*, vol. 5, p. 35, Jun. 2017.

[5] M. Bauer, J. W. Cox, M. H. Caveness, J. J. Downs, and N. F. Thornhill, "Finding the Direction of Disturbance Propagation in a Chemical Process Using Transfer Entropy," *IEEE Transactions on Control Systems Technology*, vol. 15, no. 1, pp. 12–21, 2007.

[6] B. J. Wakefield, B. S. Lindner, J. T. McCoy, and L. Auret, "Monitoring of a simulated milling circuit: Fault diagnosis and economic impact," *Minerals Engineering*, vol. 120, pp. 132–151, 2018.

[7] Y. Shu and J. Zhao, "Data-driven causal inference based on a modified transfer entropy," *Computer Aided Chemical Engineering*, vol. 31, pp. 1256–1260, 2012.

[8] R. Landman and S. L. Jamsa-Jounela, "Hybrid approach to casual analysis on a complex industrial system based on transfer entropy in conjunction with process connectivity information," *Control Engineering Practice*, vol. 53, pp. 14–23, 2016.

[9] E. Naghoosi, B. Huang, E. Domlan, and R. Kadali, "Information transfer methods in causality analysis of process variables with an industrial application," *Journal of Process Control*, vol. 23, no. 9, pp. 1296–1305, 2013.

[10] P. Hajihosseini, K. Salahshoor, and B. Moshiri, "Process fault isolation based on transfer entropy algorithm," *ISA Transactions*, vol. 53, no. 2, pp. 230–240, 2014.

[11] P. Duan, F. Yang, T. Chen, and S. L. Shah, "Direct Causality Detection via the Transfer Entropy Approach," *IEEE Transactions on Control Systems Technology*, 2013.

[12] P. Duan, F. Yang, S. Shah, and T. Chen, "Transfer Zero-Entropy and Its Application for Capturing Cause and Effect Relationship Between Variables," *IEEE Transactions on Control Systems Technology*, vol. 23, no. 3, pp. 855–867, 2015.

[13] B. Lindner, M. Chioua, J. W. D. Groenewald, L. Auret, and M. Bauer, "Diagnosis of Oscillations in an Industrial Mineral Process Using Transfer Entropy and Nonlinearity Index," in *Proceedings of the 10th IFAC Symposium on Fault Detection, Supervision and Safety for Technical Processes*, Warsaw, Poland, 2018.

[14] R. Landman, J. Kortela, Q. Sun, and S. L. Jamsa-Jounela, "Fault propagation analysis of oscillations in control loops using data-driven causality and plant connectivity," *Computers & Chemical Engineering*, vol. 71, pp. 446–456, Dec. 2014.

[15] T. Yuan and S. J. Qin, "Root cause diagnosis of plant-wide oscillations using Granger causality," *Journal of Process Control*, vol. 24, no. 2, pp. 450–459, 2014.

[16] L. Zhang, J. Zheng, and C. Xia, "Propagation Analysis of Plant-Wide Oscillations Using Partial Directed Coherence," *Journal of Chemical Engineering of Japan*, vol. 48, no. 9, pp. 766–773, 2015.

[17] M. Bauer and N. F. Thornhill, "A practical method for identifying the propagation path of plant-wide disturbances," *Journal of Process Control*, vol. 18, no. 78, pp. 707–719, Aug. 2008.

[18] L. Luo, F. Cheng, T. Qiu, and J. Zhao, "Refined convergent cross-mapping for disturbance propagation analysis of chemical processes," *Computers & Chemical Engineering*, vol. 106, pp. 1–16, 2017.

[19] C. Kuhnert, "Data-driven Methods for Fault Localization in Process Technology," PhD Thesis, KIT Scientific Publishing, Karlsruhe, 2013.

[20] C. Kuhnert and J. Beyerer, "Data-Driven Methods for the Detection of Causal Structures in Process Technology," *Machines*, vol. 2, no. 4, pp. 255–274, Nov. 2014.

[21] Y. Zhang, Y. Cen, and G. Luo, "Causal direction inference for network alarm analysis," *Control Engineering Practice*, vol. 70, pp. 148–153, Jan. 2018.

[22] N. Wiener, "The theory of prediction," *Modern mathematics for engineers*, vol. 1, pp. 125–139, 1956.

[23] H. Kantz and T. Schreiber, *Nonlinear Time Series Analysis*. New York, USA: Cambridge University Press, 1997.

[24] A. Renyi, "On Measures of Entropy and Information," in *Proceedings of the Fourth Berkeley Symposium on Mathematical Statistics and Probability, Volume 1: Contributions to the Theory of Statistics*, ser. Fourth Berkeley Symposium on Mathematical Statistics and Probability. California: University of California Press, 1961, pp. 547–561.

[25] B. Rashidi, D. S. Singh, and Q. Zhao, "Data-driven root-cause fault diagnosis for multivariate non-linear processes," *Control Engineering Practice*, vol. 70, pp. 134–147, Jan. 2018.

[26] H. Madsen, *Time series analysis*. Boca Raton: Boca Raton : Chapman & Hall/CRC, 2008.

[27] R. C. Hill, *Principles of econometrics*, 4th ed., W. E. Griffiths and G. C. G. C. Lim, Eds. Hoboken, NJ: Hoboken, NJ : Wiley, 2011.

[28] H. Akaike, "A New Look at the Statistical Model Identification," *IEEE Transactions on Automatic Control*, vol. 19, no. 6, pp. 716–723, 1974.

[29] S. L. Bressler and A. K. Seth, "Wiener - Granger Causality: A well established methodology," *NeuroImage*, vol. 58, no. 2, pp. 323–329, Sep. 2011.

[30] H.-S. Chen, Z. Yan, Y. Yao, T.-B. Huang, and Y.-S. Wong, "Systematic Procedure for Granger-Causality-Based Root Cause Diagnosis of Chemical Process Faults," *Industrial & Engineering Chemistry Research*, vol. 57, no. 29, pp. 9500–9512, Jul. 2018.

[31] G. Li, S. Qin, and T. Yuan, "Data-driven root cause diagnosis of faults in process industries," *Chemometrics and Intelligent Laboratory Systems*, vol. 159, pp. 1–11, 2016.

[32] K. Sugiyama, S. Tagawa, and M. Toda, "Methods for Visual Understanding of Hierarchical System Structures," *IEEE Transactions on Systems, Man, and Cybernetics*, vol. 11, no. 2, pp. 109–125, Feb. 1981.

[33] B. Lindner, L. Auret, and M. Bauer, "A systematic workflow for oscillation diagnosis using transfer entropy," *IEEE Transactions on Control Systems Technology*, 2018, manuscipt accepted for final submission.

[34] L. H. Chiang, B. Jiang, X. Zhu, D. Huang, and R. D. Braatz, "Diagnosis of multiple and unknown faults using the causal map and multivariate statistics," *Journal of Process Control*, vol. 28, pp. 27–39, Apr. 2015.

[35] J. Shiozaki, H. Matsuyama, E. O'Shima, and M. Iri, "An improved algorithm for diagnosis of system failures in the chemical process," *Computers and Chemical Engineering*, vol. 9, no. 3, pp. 285–293, 1985.

[36] J. Pearl, "Causal inference in statistics: An overview," *Statistics Surveys*, vol. 3, pp. 96–146, 2009.

[37] J. Bang-Jensen, *Digraphs : theory, algorithms, and applications*, 2nd ed., G. Gutin, Ed. London: London : Springer, 2010.

[38] P. Duan, "Information Theory-based Approaches for Causality Analysis with Industrial Applications," Thesis, University of Alberta, 2014.
[39] B. A. B. A. Wills, *Wills' mineral processing technology an introduction to the practical aspects of ore treatment and mineral recovery*, 7th ed., B. A. B. A. Wills, T. Napier-Munn, and Julius Kruttschnitt Mineral Research Centre, Eds. Amsterdam: Amsterdam : Elsevier Science & Technology, 2007.
[40] J. T. Lizier, "JIDT: An information-theoretic toolkit for studying the dynamics of complex systems," *Frontiers in Robotics and AI*, vol. 1, Dec. 2014.
[41] D. Marinazzo, M. Pellicoro, and S. Stramaglia, "Kernel method for nonlinear granger causality," *Physical Review Letters*, vol. 100, no. 14, p. 144103, Apr. 2008.
[42] N. Thornhill, "Finding the source of nonlinearity in a process with plant-wide oscillation," *IEEE Transactions on Control Systems Technology*, vol. 13, no. 3, pp. 434–443, 2005.
[43] B. Girod, *Signals and systems*. Chichester: Wiley, 2001.
[44] B. S. Lindner and L. Auret, "Data-driven fault detection with process topology for fault identification," *IFAC Proceedings Volumes*, vol. 47, no. 3, pp. 8903–8908, 2014.
[45] B. Lindner and L. Auret, "Application of data-based process topology and feature extraction for fault diagnosis of an industrial platinum group metals concentrator plant," *IFAC-PapersOnLine*, vol. 28, no. 17, pp. 102–107, 2015.
[46] B. Lindner, L. Auret, and N. Knoblauch, "Exploiting process topology for fault diagnosis in a simulated pressure leaching system," in *Proceedings of International Minerals Processing Conference (IMPC 2014)*, Santiago, Chile, 2014.
[47] B. Lindner, L. Auret, and M. Bauer, "Investigating the Impact of Perturbations in Chemical Processes on Data-Based Causality Analysis. Part 2: Testing Granger Causality and Transfer Entropy," *IFAC-PapersOnLine*, vol. 50, no. 1, pp. 3275–3280, 2017.
[48] ——, "Investigating the Impact of Perturbations in Chemical Processes on Data-Based Causality Analysis. Part 1: Defining Desired Performance of Causality Analysis Techniques," *IFAC-PapersOnLine*, vol. 50, no. 1, pp. 3269–3274, 2017.

APPENDIX A
TRANSFER ENTROPY APPLICATION PROCEDURE

Lindner et al. [33] presented a systematic workflow for the application of transfer entropy for diagnosis of plant-wide oscillations. This workflow was used to analyse the oscillations discussed in Section VI.

A. Detect fault

Oscillations were observed in the mass pull variable. These oscillations persisted for over 12 hours. To find the possible suspect variables one can look at upstream and downstream sections to determine whether any of their KPIs showed oscillations. Upstream of the flotation circuit is the milling circuit.

B. Perform spectral analysis

Once the oscillation has been detected, additional information on the nature of the oscillation may be discerned using spectral analysis. Using the fast-Fourier transform to find the peak oscillation frequencies it was observed that 27 of the selected trends displayed a common oscillation period of 69 min.

- **Oscillatory variables:** The variables that shared this oscillation period are shown in Figure 9. This includes variables from the primary milling circuit, flotation circuit, and secondary milling circuit.
- **Oscillation period:** $P = 69min$.

C. Select data for transfer entropy

The suspect variables identified in the variable selection step included variables from the primary milling, flotation, and secondary milling circuit.

- **Sampling time:** $T_S = 10s$.
- **Number of samples:** $N_S = 4530$ samples.
- **Suspect variables:** 27 variables shown in Figure 9.

D. Determine process dynamics

Suspect variables were narrowed down during the spectral analysis. For each pair of these variables, system identification was performed to fit a first order plus time delay model. This basic model gave a rough estimate of the time constants of the time delays between the variables. The *System Identification Toolbox* in MATLAB was used to determine the time delay estimates (T_D, in seconds) for each pair of candidate variables.

E. Select parameters for transfer entropy

The time delay and the oscillation period can be used to get parameters for transfer entropy.

$$\hat{\tau}_{max} = 0.33P + 0.53T_D + 0.66 \tag{10}$$

- **Embedding dimension for input:** $K = 1$.
- **Embedding dimension for output:** $L = 2$.
- **Time interval:** The time interval can be calculated from T_D and P using Equation 10.
- **Prediction horison:** $H = \tau$.

F. Perform transfer entropy analysis

Once all the parameters have been selected for each pair of variables the transfer entropy analysis can be performed. The causality map shown in Figure 10 was obtained.